

Duality between partial coherence and partial entanglement

Bahaa E. A. Saleh,* Ayman F. Abouraddy, Alexander V. Sergienko, and Malvin C. Teich
*Quantum Imaging Laboratory,† Department of Electrical and Computer Engineering, Boston University,
 8 Saint Mary's Street, Boston, Massachusetts 02215*

(Received 23 December 1999; published 19 September 2000)

Entangled-photon pairs (biphotons) generated by spontaneous optical parametric down-conversion exhibit a number of properties that are analogous to those of ordinary photons generated by incoherent sources. The spatial pump-field distribution and the two-particle wave function in the biphoton case play the respective roles of the source intensity distribution and the second-order coherence function in the incoherent case. The van Cittert–Zernike theorem, which is applicable for incoherent optical sources emitting independent photons, has a counterpart for biphotons. Likewise, the partial-coherence theory of image formation has an analogous counterpart for biphoton beams transporting spatial information. However, an underlying duality, rather than analogy, accompanies the mathematical similarity between incoherent and biphoton emissions if the comparison is made between the photon count rate in the incoherent case and the biphoton count rate in the entangled-photon case. The smaller the size of an incoherent source, the more separable is the coherence function and the more coherent is the field, and therefore the higher the visibility of ordinary interference fringes. In contrast, the narrower the size of a biphoton pump source, the more separable is the wave function and the less entangled is the field, and therefore the lower the visibility of biphoton interference fringes. This duality is similar to the complementarity between single and two-photon interference exhibited for biphotons.

PACS number(s): 42.50.Dv, 42.65.Ky

I. INTRODUCTION

Spontaneous parametric down-conversion (SPDC) is a weak nonlinear optical process that takes place via a three-wave interaction [1]. A coherent light wave entering a nonlinear optical medium results in the generation of two light waves of longer wavelengths; conservation of energy and momentum govern the properties of the down-converted waves [2–4]. A standard laboratory source of such nonclassical light comprises a highly monochromatic pump laser emitting light that is passed through an anisotropic optical crystal endowed with a quadratic nonlinear susceptibility $\chi^{(2)}$ [5]. By virtue of the conservation principles that govern their creation, the down-converted beams are quantum-mechanically correlated [6] and are therefore referred to as twin beams. Down-converted photon pairs are also called “biphotons,” an appellation first put forth by Klyshko [7]. Although the down-converted photon pairs are created nearly simultaneously [8], the marginal photon occurrence times, as well as the coincidence occurrences, behave as Poisson point processes [9]. The pairs are said to be entangled because the quantum state that characterizes the biphoton field is nonseparable [10].

Depending on the configuration of the experiment and the cut of the crystal, the photon pairs can be entangled in any number of variables: time, frequency, direction of propagation, and polarization [11]. Because of their remarkable properties, entangled-photon beams have found use in a broad variety of experiments that stretch from the fundamental to the applied. Studies carried out with twin-photon beams range from the examination of quantum paradoxes

[12–14] to applications in optical measurements [7,15–18], communications [19], single-photon range finding [20], spectroscopy [21], and quantum information [22,23]. In many of these experiments the down-converted beams are split and recombined with the help of beam splitters in a variety of interferometric configurations [4,11,13,14,18,22–26].

A number of these and other papers [25–31] have emphasized the spatial and spatiotemporal correlations of SPDC biphoton beams, and several imaging applications have been proposed and demonstrated [27,30,32–34]. In those applications where spatial information is transported by optical beams, both diffraction and transverse correlation effects govern the resolution.

In this paper we demonstrate that the theory of spatial correlation of biphoton beams is mathematically analogous to the coherence theory of ordinary light sources. Moreover, we show that biphoton counterparts emerge for such well-known relationships as the van Cittert–Zernike theorem and, indeed, for the quantum theory of partial coherence [4,35,36]. Furthermore, because of the similarity of the laws describing the propagation of photons and biphotons through optical systems, the behavior of ordinary incoherent light in such systems has its counterpart for down-converted light.

The mathematical *analogy* between biphoton optics and its ordinary “single-photon” counterpart becomes obvious when the biphoton wave function (representing the probability amplitude of the two-photon field) is regarded as the analog of the second-order coherence function. However, if the comparison is made between the biphoton rate and the photon rate in ordinary optics, then the result is a *duality* much like the complementarity between single- and two-photon interference in biphoton optics. This duality (rather than analogy) has the following origin: separability of the second-order coherence function is associated with the *presence of*

*Electronic address: besaleh@bu.edu

†URL: <http://www.bu.edu/qil>

coherence and thereby high-visibility ordinary interference fringes, whereas separability in the biphoton wave function is associated with the *absence of entanglement which results in low-visibility biphoton interference fringes*.

For purposes of reference and comparison, a brief overview of the well-known equations of the theory of partial coherence for photons is presented in Sec. II. A simplified version of the corresponding partial-entanglement theory for biphotons is developed in Sec. III, under the restrictions that the nonlinear crystal is thin and that the signal and idler waves are passed through narrow-band filters so that the emerging beams are quasimonochromatic. The analogy with quasimonochromatic partial-coherence theory is most obvious in this regime. Temporal and spectral effects on partial coherence and partial entanglement, and the effects of source thickness, are considered in Secs. IV and V, respectively. Throughout the paper we consider two elementary optical-system constructs: the Fourier transform ($2-f$) system, which lies at the heart of Fourier optics, and the imaging ($4-f$) system, which serves as a generic linear shift-invariant system that exhibits diffraction or interference depending on the nature of the aperture.

II. PARTIAL COHERENCE THEORY FOR PHOTONS

The theory of optical coherence is well established [4,35,36]. We provide here an overview of its basic equations for reference throughout this paper.

A. Coherence and separability

For a quasimonochromatic optical field, coherence in the second order is characterized by the coherence function $G^{(1)}(\mathbf{x}_1, \mathbf{x}_2) = \langle \hat{E}^-(\mathbf{x}_1) \hat{E}^+(\mathbf{x}_2) \rangle$, where $\hat{E}^+(\mathbf{x})$ and $\hat{E}^-(\mathbf{x})$ are the positive- and negative-frequency components of the electric field operator at the position \mathbf{x} in some plane, and $\langle \cdot \rangle$ indicates ensemble averaging. The field is said to be completely coherent if, and only if, the function $G^{(1)}(\mathbf{x}_1, \mathbf{x}_2)$ is separable. A partially coherent field can generally be expanded as a superposition of coherent (separable) contributions (modes),

$$G^{(1)}(\mathbf{x}_1, \mathbf{x}_2) = \sum_n \mu_n \varphi_n^*(\mathbf{x}_1) \varphi_n(\mathbf{x}_2), \quad (2.1)$$

where the functions $\varphi_n(\mathbf{x})$ and the parameters μ_n are appropriate eigenfunctions and eigenvalues. A single-mode field is separable (completely coherent), whereas a multimode field is nonseparable (partially coherent). A completely incoherent field, for which $G^{(1)}(\mathbf{x}_1, \mathbf{x}_2) \propto \delta(\mathbf{x}_1 - \mathbf{x}_2)$, is characterized by a uniformly weighted superposition of modes (equal eigenvalues).

B. Propagation

Consider quasimonochromatic light emitted from a thin planar light source, transmitted through an arbitrary linear optical system, and observed at some observation plane, as illustrated in Fig. 1. If $h(x_1, x)$ is the impulse response function of the system, then the second-order coherence function

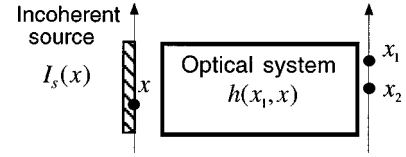


FIG. 1. Propagation of light emitted from an incoherent source through a linear optical system of impulse response function $h(x_1, x)$.

at the output plane, $G^{(1)}(x_1, x_2)$, is related to the second-order coherence function at the source plane, $G_s^{(1)}(x, x')$, by

$$G^{(1)}(x_1, x_2) = \int \int G_s^{(1)}(x, x') h^*(x_1, x) h(x_2, x') dx dx'. \quad (2.2)$$

The range of the integrals is $[-\infty, \infty]$ throughout, unless otherwise indicated. For simplicity, we assume that x is one dimensional; generalization to the two-dimensional case is straightforward. If the source field is completely incoherent, i.e., $G_s^{(1)}(x, x') = I_s(x) \delta(x - x')$, where $I_s(x)$ is the source intensity, then,

$$G^{(1)}(x_1, x_2) = \int I_s(x) h^*(x_1, x) h(x_2, x) dx, \quad (2.3)$$

from which

$$G^{(1)}(x_1, x_2) = \frac{1}{4\pi^2} \int \int \tilde{I}_s(q_1 - q_2) H^*(x_1, q_1) \times H(x_2, q_2) dq_1 dq_2, \quad (2.4)$$

where $\tilde{I}_s(q) = \int I_s(x) e^{-iqx} dx$ is the Fourier transform of $I_s(x)$ and $H(x_1, q)$ is the Fourier transform of $h(x_1, x)$ with respect to $-x$.

Equation (2.3) represents a continuous modal expansion similar to that in Eq. (2.1) with the summation index n replaced by the variable x , and the eigenvalues μ_n replaced by the source function $I_s(x)$. It follows that each point of the source creates its own coherent mode. If the source itself is a single point [$I_s(x) \propto \delta(x)$], we have a single mode with a separable, and hence completely coherent, field. As the source size increases, the number of modes increases, the ‘‘separability’’ diminishes, and coherence is reduced.

The optical intensity at the output plane, $I(x_1) = G^{(1)}(x_1, x_1)$, which is proportional to the rate of photon arrivals, is a linear transformation of the source intensity,

$$I(x_1) = \int dx I_s(x) |h(x_1, x)|^2. \quad (2.5)$$

C. van Cittert–Zernike theorem

For the Fourier-transform optical system depicted in Fig. 2(a), called a $2-f$ system, $h(x_1, x) \propto \exp[-i2\pi(x_1/\lambda f)x]$, where λ is the wavelength of the light and f is the focal length of the lens. In this case Eq. (2.3) gives

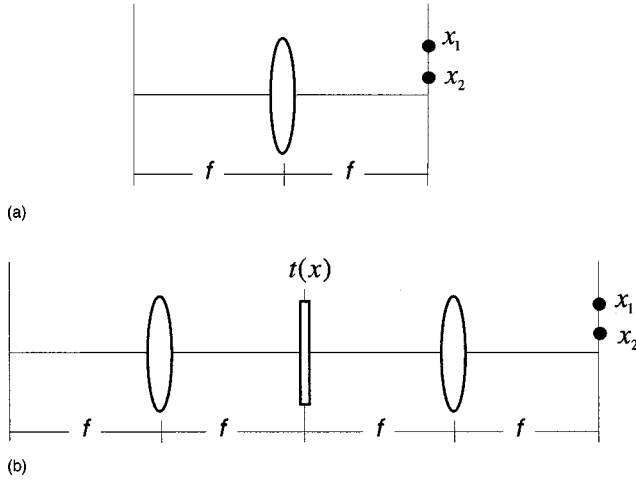


FIG. 2. (a) 2- f (Fourier-transform) optical system. (b) 4- f (imaging) optical system with an aperture $t(x)$ placed in the Fourier plane.

$$G^{(1)}(x_1, x_2) \propto \int I_s(x) \exp\left(-i2\pi \frac{x_2 - x_1}{\lambda f} x\right) dx = \tilde{I}_s\left(2\pi \frac{x_2 - x_1}{\lambda f}\right), \quad (2.6)$$

where $\tilde{I}_s(q)$ is the Fourier transform of $I_s(x)$. Equation (2.6) is known as the van Cittert–Zernike theorem and is the basis of a well-known technique for measurement of the angular diameters of stars [4].

D. Diffraction and interference

For a 4- f system with an aperture $t(x)$ placed at the Fourier plane, as illustrated in Fig. 2(b), the impulse response function is $h(x_1, x) \propto T[2\pi(x - x_1)/\lambda f]$ where $T(q)$ is the Fourier transform of $t(x)$, and the axes at the output plane are inverted with respect to the input plane, so that Eq. (2.3) yields

$$G^{(1)}(x_1, x_2) \propto \int I_s(x) T^*\left(2\pi \frac{x - x_1}{\lambda f}\right) T\left(2\pi \frac{x - x_2}{\lambda f}\right) dx. \quad (2.7)$$

For a point source $I_s(x) \propto \delta(x)$, the coherence function $G^{(1)}(x_1, x_2) \propto T^*(-2\pi x_1/\lambda f) T(-2\pi x_2/\lambda f)$ is separable, and the corresponding intensity $I(x_1) \propto |T(-2\pi x_1/\lambda f)|^2$ is the diffraction pattern created by the aperture $t(x)$ when illuminated by a coherent source.

For a double-slit aperture with slits separated by a distance a , $t(x) = \delta(x - a/2) + \delta(x + a/2)$, and Eq. (2.7) gives

$$G^{(1)}(x_1, x_2) \propto \left[S_1 \cos\left(\pi \frac{x_1 + x_2}{\Lambda}\right) + \cos\left(\pi \frac{x_1 - x_2}{\Lambda}\right) \right], \quad (2.8)$$

where $\Lambda = \lambda/\theta$ is the fringe period, $\theta = a/f$ is the angle subtended by the pinholes, and $S_1 = \tilde{I}_s(1/\Lambda)/\tilde{I}_s(0)$. The corresponding intensity $I(x_1) = G^{(1)}(x_1, x_1)$ is

$$I(x_1) \propto \left[1 + S_1 \cos\left(2\pi \frac{x_1}{\Lambda}\right) \right], \quad (2.9)$$

which is an interference pattern with visibility

$$V_{\text{inc}} = S_1 = \frac{\tilde{I}_s(\Lambda^{-1})}{\tilde{I}_s(0)}. \quad (2.10)$$

The subscript ‘‘inc’’ is used to denote incoherent light.

For a light source of uniform intensity confined within an area of width b , $S_1 = \text{sinc}(b/\Lambda)$, where $\text{sinc}(x) \equiv \sin(\pi x)/\pi x$. In the limit of a small source ($b \ll \Lambda$), the light at the slit plane is coherent and the visibility $V_{\text{inc}} = S_1 \rightarrow 1$, whereas in the opposite limit of a large source ($b \gg \Lambda$) the light at the slit is incoherent, and the visibility $V_{\text{inc}} = S_1 \rightarrow 0$.

E. Fourth-order coherence function

The coincidence rate of photoevents detected at the positions x_1 and x_2 is proportional to the fourth-order coherence function $G^{(2)}(x_1, x_2) = \langle \hat{E}^-(x_1) \hat{E}^-(x_2) \hat{E}^+(x_2) \hat{E}^+(x_1) \rangle$. If the incoherent light is thermal (which used to be referred to as chaotic), the rate of photon coincidences is related to the second-order coherence function by the Siegert relation [37],

$$G_{\text{th}}^{(2)}(x_1, x_2) = G^{(1)}(x_1, x_1) G^{(1)}(x_2, x_2) + |G^{(1)}(x_1, x_2)|^2, \quad (2.11)$$

where the subscript ‘‘th’’ is used to denote incoherent thermal light. This equation is the basis of the Hanbury-Brown–Twiss effect [4,35]. A fundamental difficulty in observing this effect is the small relative magnitude of the second term on the right-hand side of Eq. (2.11) when the coherence time of the detected field is much smaller than the detection time interval. As will be shown in Sec. IV, this term then turns out to be multiplied by a small factor (the ratio of the two times), so that it becomes difficult to observe in the presence of an undiminished first term [37].

It is therefore useful to define an excess fourth-order coherence function

$$\Delta G_{\text{th}}^{(2)}(x_1, x_2) = G_{\text{th}}^{(2)}(x_1, x_2) - G^{(1)}(x_1, x_1) G^{(1)}(x_2, x_2). \quad (2.12)$$

This function vanishes if the photons arrive independently at x_1 and x_2 , as is the case for a coherent field. For a thermal source, Eq. (2.12) becomes

$$\Delta G_{\text{th}}^{(2)}(x_1, x_2) = |G^{(1)}(x_1, x_2)|^2. \quad (2.13)$$

III. PARTIAL ENTANGLEMENT THEORY FOR BIPHOTONS

We now consider light generated by spontaneous parametric down-conversion from a thin planar nonlinear crystal and examine its transmission through the same systems described in Sec. II. Here, the light is generated in the form of photon pairs, denoted as the signal and idler, emitted from a

common position within the nonlinear crystal. Although the direction of each photon of a pair is random, it is highly correlated with the direction of its twin by virtue of conservation of momentum.

A. Entanglement and separability

The two-photon field is characterized by the state $|\Psi\rangle$ or the wave function $\psi(x_1, x_2) = \langle 0, 0 | \hat{E}^+(x_2) \hat{E}^+(x_1) | \Psi \rangle$, where $|0, 0\rangle$ is the vacuum state. The state is said to be entangled if the function $\psi(x_1, x_2)$ is *not* separable. Using a modal expansion similar to that in Eq. (2.1), this function may be written as a superposition of separable functions,

$$\psi(x_1, x_2) = \sum_n \eta_n \psi_{1n}^*(x_1) \psi_{2n}(x_2). \quad (3.1)$$

The single-mode case corresponds to a separable (nonentangled) state, while the multimode case describes a partially entangled state. The index n may represent the frequency, wave vector, or polarization of the mode. The probability of coincidence of photons at the positions x_1 and x_2 , $G^{(2)}(x_1, x_2) = \langle \Psi | \hat{E}_1^-(x_1) \hat{E}_2^-(x_2) \hat{E}_2^+(x_2) \hat{E}_1^+(x_1) | \Psi \rangle$, is simply the square magnitude of the two-photon wave function:

$$G^{(2)}(x_1, x_2) = |\psi(x_1, x_2)|^2. \quad (3.2)$$

The marginal rate of single-photon arrivals $G^{(1)}(x_1, x_1)$ may be obtained by integrating $G^{(2)}(x_1, x_2)$ with respect to x_2 . As in Eq. (2.12), it is useful to define the excess fourth-order coherence function (excess biphoton rate)

$$\Delta G^{(2)}(x_1, x_2) = G^{(2)}(x_1, x_2) - G^{(1)}(x_1, x_1) G^{(1)}(x_2, x_2), \quad (3.3)$$

which is the coincidence rate in excess of that expected if the particles were independent (unentangled).

B. Propagation

Consider SPDC light emitted from a planar thin nonlinear crystal (NLC) illuminated by a pump beam with transverse electric-field distribution $E_p(x)$. The emitted signal and idler beams are transmitted through separate optical systems, with impulse response functions $h_s(x_1, x)$ and $h_i(x_2, x)$, and are detected by detectors \mathcal{D}_1 and \mathcal{D}_2 , respectively. The arrival of the photon pair at positions x_1 and x_2 in the output plane is observed by measuring the coincidence rate (or biphoton rate) $G^{(2)}(x_1, x_2)$. The system is illustrated schematically in Fig. 3.

It can be shown (see the Appendix) that the two-photon wave function is given by

$$\psi(x_1, x_2) \propto \int E_p(x) h_s(x_1, x) h_i(x_2, x) dx. \quad (3.4)$$

A special case of this formula when the signal and idler systems comprise free-space propagation was developed previously [38]. The physics underlying Eq. (3.4) may be elucidated in the Fourier-transform domain (momentum space).

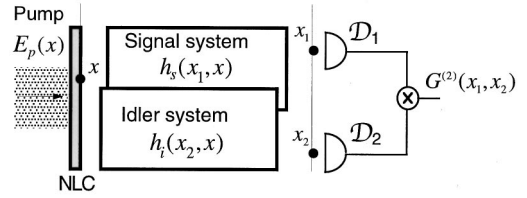


FIG. 3. Biphotons generated in a nonlinear crystal (NLC) are transmitted through a pair of linear optical systems and detected by a coincidence counter.

Expanding each of the three spatial functions in the integrand in terms of its Fourier transform, we write Eq. (3.4) in the form

$$\psi(x_1, x_2) \propto \iint \tilde{E}_p(q_s + q_i) H_s(x_1, q_s) H_i(x_2, q_i) dq_s dq_i, \quad (3.5)$$

where $\tilde{E}_p(q)$ is the Fourier transform of $E_p(x)$, $H_s(x_1, q_s)$ is the Fourier transform of $h_s(x_1, x)$ with respect to $-x$, and $H_i(x_2, q_i)$ is similarly defined. The function $\tilde{E}_p(q)$ is the amplitude of a pump plane-wave component traveling in a direction corresponding to the spatial frequency q . It is evident from Eq. (3.5) that the signal and idler plane waves, with spatial frequencies q_s and q_i , are coupled to the pump plane-wave component with spatial frequency $q = q_s + q_i$, indicating conservation of momentum in the transverse direction. Since the nonlinear crystal is assumed to be thin, momentum conservation in the longitudinal direction is not invoked. This limitation will be removed in Sec. V.

C. Comparison between incoherent thermal and SPDC light

For an ordinary incoherent light source the second-order coherence function $G^{(1)}(x_1, x_2)$ is given by Eq. (2.3), while for SPDC light the biphoton wave function $\psi(x_1, x_2)$ is given by Eq. (3.4). The similarity between these two equations is striking. In this analogy, the pump field $E_p(x)$ plays the role of the source intensity $I_s(x)$, and, except for a conjugation operation in the incoherent case [Eq. (2.3)], the impulse response functions of the optical systems play similar roles. If the incoherent source is thermal, then in view of the Siegert relation, the excess coincidence rate [Eq. (2.13)] is $\Delta G_{\text{th}}^{(2)}(x_1, x_2) = |G^{(1)}(x_1, x_2)|^2$, whereas in the SPDC case, the photon coincidence rate [Eq. (3.2)] is $G^{(2)}(x_1, x_2) = |\psi(x_1, x_2)|^2$. The fourth-order coherence function for a thermal source is therefore distinguished only by a background term, which typically dominates Eq. (2.11) as discussed earlier. This background term is absent in the biphoton case, as has been recognized by Belinsky and Klyshko [26]. In view of this, we conclude that every conventional system making use of thermal light has an analogous biphoton system.

Another perspective for comparing the two light sources is to regard the biphoton rate in the SPDC case [Eqs. (3.2) and (3.4)] as the dual to the single-photon rate in the incoherent case [Eq. (2.5)]. From this perspective, the effect of

the spatial distribution of the source $I_s(x)$ in the incoherent case is opposite that of the pump spatial distribution $E_p(x)$ in the biphoton case. It is immediately evident from Eq. (2.5) that the smaller the width of the incoherent source $I_s(x)$, the more ‘‘coherent’’ is the emitted light; indeed when the source is reduced to a point, the emitted light is completely coherent and its second-order coherence function at any location within the system is separable [as can also be seen from Eq. (2.3)]. Therefore, if two slits are placed within the system, the resultant Young’s interference fringes will have high visibility. In contrast, it is evident from Eq. (3.4) that the wider the pump beam $E_p(x)$ in the biphoton case, the more ‘‘entangled’’ are the emitted signal and idler photons. If the pump beam is reduced to a point, the wave function $\psi(x_1, x_2)$ factors, and the emitted light is unentangled; the visibility of biphoton (fourth-order) interference fringes (visibility as a function of $x_1 - x_2$) then vanishes. A quantitative derivation of this effect is provided later in this section, and several examples highlighting the duality are provided.

D. Biphoton van Cittert–Zernike theorem

If each of the signal and idler systems separately comprises a 2- f optical system, as illustrated in Fig. 2(a), then $h_s(x_1, x) \propto \exp(-i2\pi(x_1 x)/\lambda_s f)$ and $h_i(x_2, x) \propto \exp(-i2\pi(x_2 x)/\lambda_i f)$, so that Eqs. (3.4) and (3.2) provide

$$G^{(2)}(x_1, x_2) \propto \left| \tilde{E}_p \left[\frac{2\pi}{f} \left(\frac{x_1}{\lambda_s} + \frac{x_2}{\lambda_i} \right) \right] \right|^2, \quad (3.6)$$

where $\tilde{E}_p(q)$ is the Fourier transform of $E_p(x)$. This equation is the biphoton version of the classical van Cittert–Zernike theorem, Eq. (2.6).

There are distinctions between the two theorems. The pump field in the biphoton case plays the role of the source intensity in the incoherent case. The pump field is, of course, a complex function whose phase may introduce interesting effects that are not present in the incoherent case. Moreover, in the biphoton case, the argument of the Fourier transform is proportional to $(x_1/\lambda_s + x_2/\lambda_i)$ instead of $(x_1/\lambda - x_2/\lambda)$. For example, if the source is of uniform intensity and of width b , then in the incoherent case $G^{(1)}(x_1, x_2)$ is a sinc function of width $\lambda f/b$ centered at $x_2 = x_1$. In the biphoton case, for a uniform pump beam of width b traveling in the longitudinal direction, and assuming that $\lambda_s = \lambda_i = \lambda$, the biphoton rate $G^{(2)}(x_1, x_2)$ is a sinc² function of width $\lambda f/b$ centered at $x_2 = -x_1$, where $\text{sinc}(x) = \sin(\pi x)/\pi x$. If the pump beam is tilted by a small angle θ , i.e., if $E_p(x)$ is modified by a phase factor $(2\pi/\lambda_p)\theta x = (2\pi/\lambda)(2\theta)x$, then the Fourier transform is shifted so that its peak is centered at $x_2 = -x_1 + 2\theta f$. The fact that the angular spectrum of the pump beam is represented in the biphoton rate is an important feature of the biphoton process [3,29,30].

E. Biphoton diffraction

If each of the signal and idler beams separately comprises a 4- f system with an aperture $t(x)$, then, in the degenerate case, $h_s(x_1, x) = h_i(x_1, x) \propto T[2\pi(x - x_1)/\lambda f]$, where $T(q)$

is the Fourier transform of $t(x)$ and λ is the wavelength of the signal/idler wave. In this case Eq. (3.4) provides

$$\psi(x_1, x_2) \propto \int E_p(x) T \left(2\pi \frac{x - x_1}{\lambda f} \right) T \left(2\pi \frac{x - x_2}{\lambda f} \right) dx, \quad (3.7)$$

which is analogous to Eq. (2.7) in the incoherent case.

For a narrow pump beam centered at $x=0$, $E_p(x) \propto \delta(x)$, and the biphoton rate $G^{(2)}(x_1, x_2) = |\psi(x_1, x_2)|^2 \propto |T[2\pi(-x_1)/\lambda f]|^2 |T[2\pi(-x_2)/\lambda f]|^2$ is separable. The light is then unentangled and the biphoton (coincidence) diffraction pattern is the product of the single-photon diffraction patterns, i.e., $\Delta G^{(2)}(x_1, x_2) = 0$. In the opposite limit of a uniform pump, $E_p(x) = \text{const}$, $G^{(2)}(x_1, x_2) \propto |T[2\pi(x_2 - x_1)/\lambda f]|^2$, where $T(q)$ is the Fourier transform of $t(x)t(-x)$. This is the fully entangled case, which represents true biphoton diffraction.

F. Biphoton interference

For a degenerate SPDC source with a pair of 4- f systems, each incorporating a double-slit aperture $t(x) = \delta(x - a/2) + \delta(x + a/2)$, Eqs. (3.7) and (3.2) give

$$\begin{aligned} G^{(2)}(x_1, x_2) &= \frac{1}{2\Lambda^2} \frac{1}{1+S_2^2} \left[S_2 \cos \left(\pi \frac{x_1 + x_2}{\Lambda} \right) \right. \\ &\quad \left. + \cos \left(\pi \frac{x_1 - x_2}{\Lambda} \right) \right]^2 \\ &= \frac{1}{4\Lambda^2} \left\{ 1 + \frac{1}{1+S_2^2} \left[S_2^2 \cos \left(2\pi \frac{x_1 + x_2}{\Lambda} \right) \right. \right. \\ &\quad \left. + \cos \left(2\pi \frac{x_1 - x_2}{\Lambda} \right) + 2S_2 \cos \left(2\pi \frac{x_1}{\Lambda} \right) \right. \\ &\quad \left. \left. + 2S_2 \cos \left(2\pi \frac{x_2}{\Lambda} \right) \right] \right\}, \quad (3.8) \end{aligned}$$

where $\Lambda = \lambda/\theta$ is the fringe period, $\theta = a/f$ is the angle subtended by the pinholes, and $S_2 = \tilde{E}_p(\Lambda^{-1})/\tilde{E}_p(0)$. The function $G^{(2)}(x_1, x_2)$ in Eq. (3.8) was normalized such that its integral with respect to x_1 and x_2 over the interval from 0 to 2Λ is 1. Since the photons are indistinguishable, the probability that the pair is found anywhere within $[0, 2\Lambda]$ is unity.

The marginal signal (or idler) photon rate associated with the joint signal-idler rate in Eq. (3.8) may be obtained by integrating $G^{(2)}(x_1, x_2)$ with respect to x_2 (or x_1) over the interval 0 to 2Λ , yielding

$$G^{(1)}(x_1, x_1) = \frac{1}{2\Lambda} \left[1 + \frac{2S_2}{1+S_2^2} \cos \left(2\pi \frac{x_1}{\Lambda} \right) \right]. \quad (3.9)$$

A similar expression for $G^{(1)}(x_2, x_2)$ is obtained. The visibility of this interference pattern is

$$V_1 = 2|S_2|/(1+S_2^2). \quad (3.10)$$

When the pump beam has a uniform distribution that is confined to an aperture of width b , $S_2 = \text{sinc}(b/\Lambda)$. For a pump beam of large width ($b \gg \Lambda$), $S_2 \rightarrow 0$, and

$$G^{(2)}(x_1, x_2) = \frac{1}{4\Lambda^2} \left[1 + \cos\left(2\pi \frac{x_1 - x_2}{\Lambda}\right) \right], \quad (3.11)$$

which is a fourth-order interference pattern of unity visibility. This corresponds to the fully entangled limit. In the opposite limit of a pump beam of narrow width ($b \ll \Lambda$), $S_2 \rightarrow 1$, whereupon the biphoton rate becomes

$$G^{(2)}(x_1, x_2) = \frac{1}{4\Lambda^2} \left[1 + \cos\left(2\pi \frac{x_1}{\Lambda}\right) \right] \left[1 + \cos\left(2\pi \frac{x_2}{\Lambda}\right) \right], \quad (3.12)$$

which is a separable function. In this case, each of the emitted photons passes through its own slits independently and forms its own interference pattern (with unity visibility).

In the general case, we can compute the ‘‘true’’ biphoton interference by determining the excess coincidence rate $\Delta G^{(2)}(x_1, x_2)$ defined by Eq. (3.3). It turns out [39] that this subtraction also removes a constant background of $1/4\Lambda^2$, which must be added to obtain the ‘‘corrected’’ rate $\overline{\Delta G}^{(2)}(x_1, x_2) = \Delta G^{(2)}(x_1, x_2) + 1/4\Lambda^2$. Using Eqs. (3.8) and (3.9) we obtain

$$\begin{aligned} \overline{\Delta G}^{(2)}(x_1, x_2) &= \frac{1}{4\Lambda^2} \left[1 + V_{12} \sin\left(2\pi \frac{x_1}{\Lambda}\right) \sin\left(2\pi \frac{x_2}{\Lambda}\right) \right. \\ &\quad \left. + V_{12}^2 \cos\left(2\pi \frac{x_1}{\Lambda}\right) \cos\left(2\pi \frac{x_2}{\Lambda}\right) \right] \\ &= \frac{1}{4\Lambda^2} \left[1 + \frac{1}{2}(V_{12} + V_{12}^2) \cos\left(2\pi \frac{x_1 - x_2}{\Lambda}\right) \right. \\ &\quad \left. - \frac{1}{2}(V_{12} - V_{12}^2) \cos\left(2\pi \frac{x_1 + x_2}{\Lambda}\right) \right], \quad (3.13) \end{aligned}$$

where

$$V_{12} = \frac{1 - S_2^2}{1 + S_2^2}. \quad (3.14)$$

This is a fringe pattern with visibility V_{12} . The visibilities of the marginal single-photon and pure biphoton patterns, V_1 and V_{12} , respectively, are related by the complementarity relation

$$V_1^2 + V_{12}^2 = 1, \quad (3.15)$$

which is sketched in Fig. 4(a). This relation was first noted in Ref. [39].

If we now compare the visibility of biphoton fringes with the visibility of single-photon fringes V_{inc} created by an equivalent ordinary incoherent source of the same source distribution, so that the parameters $S_1 = S_2$, we find that the visibilities are related by

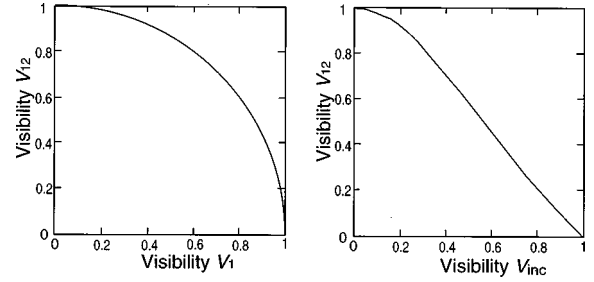


FIG. 4. (a) Visibility V_{12} of pure biphoton fringes versus visibility V_1 of marginal single-photon fringes in an interference experiment using light emitted by spontaneous parametric down-conversion. (b) Visibility V_{12} of pure biphoton fringes in an interference experiment using light emitted by spontaneous parametric down-conversion, versus visibility V_{inc} of single photons in an equivalent interference experiment using a conventional incoherent light source.

$$V_{12} = \frac{1 - V_{\text{inc}}^2}{1 + V_{\text{inc}}^2}. \quad (3.16)$$

As illustrated in Fig. 4(b), this monotonically decreasing relation is not unlike that between V_{12} and V_1 .

IV. TEMPORAL AND SPECTRAL EFFECTS IN PARTIAL COHERENCE AND PARTIAL ENTANGLEMENT

The analogy between the entanglement properties of light emitted from a SPDC source and the properties of light emitted from an incoherent source can be extended to include temporal/spectral effects and is therefore also applicable for nonmonochromatic light. We begin with a brief overview of conventional coherence theory for polychromatic light and then establish the equivalent polychromatic biphoton entanglement theory. The thin-source assumption is retained in this section.

A. Coherence theory for polychromatic incoherent sources

The coherence properties of polychromatic stationary light are described by a second-order coherence function of the form [4,35,36]

$$G^{(1)}(x_1, t_1; x_2, t_2) = \int \tilde{G}^{(1)}(x_1, x_2; \omega) e^{-i\omega(t_1 - t_2)} d\omega, \quad (4.1)$$

where $\tilde{G}^{(1)}(x_1, x_2; \omega)$ is the spectral coherence function. If the light is generated from a spatially incoherent stationary planar source with spectral coherence function

$$\tilde{G}_s^{(1)}(x, x'; \omega) = I_s(x; \omega) \delta(x - x'), \quad (4.2)$$

transmitted through a linear system with impulse response function $h(x_1, x; \omega)$ at the angular frequency ω , then

$$\tilde{G}^{(1)}(x_1, x_2; \omega) = \int I_s(x; \omega) h^*(x_1, x; \omega) h(x_2, x; \omega) dx. \quad (4.3)$$

This relation may also be written in the form,

$$\begin{aligned} \tilde{G}^{(1)}(x_1, x_2; \omega) &= \frac{1}{4\pi^2} \int \int \tilde{I}_s(q_2 - q_1; \omega) H^*(x_1, q_1; \omega) \\ &\quad \times H(x_2, q_2; \omega) dq_1 dq_2, \end{aligned} \quad (4.4)$$

where $H(x_1, q; \omega)$ is the Fourier transform of $h(x_1, x; \omega)$ with respect to the variable x , and $\tilde{I}_s(q; \omega)$ is the Fourier transform of $I_s(x; \omega)$. The intensity of the transmitted light is

$$I(x) = \int \tilde{G}^{(1)}(x, x; \omega) d\omega. \quad (4.5)$$

If the incoherent source is thermal, the rate of coincidence of a photon at (x_1, t_1) and another at (x_2, t_2) is given by the Siegert relation

$$G_{\text{th}}^{(2)}(x_1, t_1; x_2, t_2) = I(x_1)I(x_2) + |G^{(1)}(x_1, t_1; x_2, t_2)|^2. \quad (4.6)$$

If this rate is measured with detectors of resolution time T , serving as integrators, then the rate of two-photon coincidence in the interval is

$$C_{\text{th}}(x_1, x_2) \propto \frac{1}{T} \int_0^T \int_0^T G_{\text{th}}^{(2)}(x_1, t_1; x_2, t_2) dt_1 dt_2. \quad (4.7)$$

Substituting from Eq. (4.6),

$$\begin{aligned} C_{\text{th}}(x_1, x_2) &\propto I(x_1)I(x_2) + \frac{1}{T^2} \\ &\quad \times \int_0^T \int_0^T |G^{(1)}(x_1, t_1; x_2, t_2)|^2 dt_1 dt_2. \end{aligned} \quad (4.8)$$

Using Eq. (4.1) and assuming that T is much greater than the inverse of the spectral bandwidth of the light,

$$C_{\text{th}}(x_1, x_2) \propto I(x_1)I(x_2) + \frac{1}{T} \int |\tilde{G}^{(1)}(x_1, x_2; \omega)|^2 d\omega. \quad (4.9)$$

It can be shown that the ratio of the second to the first term in Eq. (4.9) is of the order of $(T\Omega)^{-1}$ where Ω is the spectral width. For $T \gg 1/\Omega$, this is a small number.

B. Entanglement theory for polychromatic biphoton sources

We now consider SPDC emission from a thin nonlinear crystal illuminated by a monochromatic pump beam of angular frequency ω_p and amplitude $E_p(x)$. The emitted signal and idler beams are assumed to travel through separate linear systems with spatial impulse response functions $h_s(x_1, x; \omega)$ and $h_i(x_1, x; \omega)$, respectively. The biphoton rate at positions x_1 and x_2 at times t_1 and t_2 ,

$$\begin{aligned} G^{(2)}(x_1, t_1; x_2, t_2) &= \langle \Psi | \hat{E}_1^-(x_1, t_1) \hat{E}_2^-(x_2, t_2) \hat{E}_2^+(x_2, t_2) \hat{E}_1^+(x_1, t_1) | \Psi \rangle, \end{aligned}$$

is related to the wave function $\psi(x_1, t_1; x_2, t_2) = \langle 0, 0 | \hat{E}_2^+(x_2, t_2) \hat{E}_1^+(x_1, t_1) | \Psi \rangle$ by

$$G^{(2)}(x_1, t_1; x_2, t_2) = |\psi(x_1, t_1; x_2, t_2)|^2, \quad (4.10)$$

where (as is shown in the Appendix)

$$\psi(x_1, t_1; x_2, t_2) = e^{-i\omega_p t_2} \int e^{-i\omega_s(t_1 - t_2)} \tilde{\psi}(x_1, x_2; \omega_s) d\omega_s \quad (4.11)$$

and

$$\tilde{\psi}(x_1, x_2; \omega_s) \propto \int E_p(x) h_s(x_1, x; \omega_s) h_i(x_2, x; \omega_p - \omega_s) dx. \quad (4.12)$$

Equation (4.12) is identical to Eq. (3.4), with the spectral dependence now explicitly identified. In the spatial Fourier domain Eq. (4.12) takes the form

$$\begin{aligned} \tilde{\psi}(x_1, x_2; \omega_s) &\propto \int \int \tilde{E}_p(q_s + q_i) H_s(x_1, q_s; \omega_s) \\ &\quad \times H_i(x_2, q_i; \omega_p - \omega_s) dq_s dq_i, \end{aligned} \quad (4.13)$$

which is identical to Eq. (3.5). Here, $\tilde{E}_p(q)$ is the Fourier transform of $E_p(x)$, $H_s(x_1, q_s; \omega_s)$ is the Fourier transform of $h_s(x_1, x; \omega_s)$ with respect to the variable x , and a similar relation applies to the idler system.

If the biphoton rate is measured with detectors that are not sufficiently fast to record the exact times of arrival of the photon pair, then the response $C(x_1, x_2)$ is given by Eq. (4.7). In the limit of large T (in comparison with the inverse of the spectral bandwidth of the signal/idler system), substitution of Eq. (4.11) into Eqs. (4.10) and (4.7) leads to

$$C(x_1, x_2) = \int |\tilde{\psi}(x_1, x_2; \omega_s)|^2 d\omega_s. \quad (4.14)$$

C. Equivalence of formulations for polychromatic incoherent and SPDC sources

Comparing Eqs. (4.3) and (4.12), we see that the spectral wave function $\tilde{\psi}(x_1, x_2; \omega_s)$, in the SPDC case, and the spectral coherence function $\tilde{G}^{(1)}(x_1, x_2; \omega)$ in the conventional case, have the same dependence on the source and the propagation systems, and therefore exhibit similar behavior. Comparing Eqs. (4.5) and (4.14), we see that in the conventional case the photon rate $I(x)$ is the spectral integral of the spectral coherence function, while in the SPDC case the biphoton rate $C(x_1, x_2)$ is the spectral integral of the squared magnitude of the spectral wave function. On the other hand, comparing Eq. (4.9) with Eq. (4.14) reveals that the biphoton (coincidence) rate is free from the large background term that is present in the conventional thermal rate.

We now proceed to examine the spectral effects for the same optical systems considered in Secs. II and III. In making this comparison, we assume that the spectral distribution of the incoherent source is uniform within a bandwidth Ω

centered about a central frequency ω_0 , i.e., $I_s(x; \omega) = I_s(x)$ for $|\omega - \omega_0| \leq \Omega/2$, and zero otherwise. Likewise, in the biphoton case, while the pump is assumed to be monochromatic at frequency ω_p , the signal and idler components of the emitted biphoton, which are generally broadband, are assumed to be passed through filters with uniform transmittance of width Ω centered about the degenerate frequency $\omega_0 = \omega_p/2$.

D. Polychromatic photon and biphoton van Cittert–Zernike theorems

For the 2- f system illustrated in Fig. 2(a), assuming that the lens and the detection system are achromatic, we have $h(x_1, x; \omega) = h_s(x_1, x; \omega) = h_i(x_1, x; \omega) \propto \exp(-i\omega x_1/cf)$. In the incoherent case, Eq. (4.3) gives

$$\tilde{G}^{(1)}(x_1, x_2; \omega) \propto \tilde{I}_s \left(\frac{\omega}{c} \frac{x_2 - x_1}{f} \right), \quad |\omega - \omega_0| \leq \Omega/2, \quad (4.15)$$

while in the biphoton case Eq. (4.12) gives

$$\begin{aligned} \tilde{\psi}(x_1, x_2; \omega_s) &\propto \tilde{E}_p \left(\frac{\omega_s}{c} \frac{x_1}{f} + \frac{\omega_p - \omega_s}{c} \frac{x_2}{f} \right) \\ &= \tilde{E}_p \left(\frac{\omega_0}{c} \frac{x_1 + x_2}{f} + \frac{\omega_s - \omega_0}{c} \frac{x_1 - x_2}{f} \right), \\ &|\omega_s - \omega_0| \leq \Omega/2. \end{aligned} \quad (4.16)$$

The essential equivalence between the conventional and biphoton sources is evident in Eqs. (4.15) and (4.16). There are differences, however. Whereas the spectral coherence function $\tilde{G}^{(1)}(x_1, x_2; \omega)$ in the conventional case is homogeneous (a function of $x_1 - x_2$), $\tilde{\psi}(x_1, x_2; \omega_s)$ is generally not homogeneous. Only the degenerate frequency component $\omega_s = \omega_0$ corresponds to a wave function that is dependent on $x_1 + x_2$, but not on $x_1 - x_2$.

At points for which $x_1 = x_2$ the spectral wave function is independent of frequency (within the filter bandwidth) so that the two-photon coincidence rate for photons arriving at the same position is given by

$$G^{(2)}(x, t_1; x, t_2) \propto \Omega^2 \left| \tilde{E}_p \left(2\pi \frac{x}{\lambda_p f} \right) \right|^2 \text{sinc}^2 \left(\frac{t_1 - t_2}{\tau_c} \right), \quad (4.17)$$

where $\tau_c = 2\pi/\Omega$. This function has a half width at half maximum of $t_1 - t_2 = 0.44\tau_c$, so that τ_c is a measure of the entanglement time. The rate of arrival of photon pairs at the same position is obtained by use of Eq. (4.14),

$$C(x, x) \propto \Omega \left| \tilde{E}_p \left(\frac{\omega_p x}{cf} \right) \right|^2. \quad (4.18)$$

This is proportional to the ordinary diffraction pattern of monochromatic coherent light at the pump frequency.

In a similar setup using an incoherent source, the rate of arrival of single photons, obtained from Eq. (4.5), is $I(x)$

$\propto \Omega \tilde{I}_s(0)$, which is independent of position. Likewise the rate of accidental arrival of photon pairs at the same point, as given by Eq. (4.8), is independent of position. In contrast, the rate of arrival of photon pairs at two different positions, as derived from Eq. (4.8), is (assuming the incoherent source is thermal)

$$\begin{aligned} C_{\text{th}}(x_1, x_2) &\propto 1 + \frac{1}{\Omega T} \\ &\times \left[\frac{1}{\Omega} \int_{\omega_0 - \Omega/2}^{\omega_0 + \Omega/2} \left| \tilde{I}_s \left(\frac{\omega}{c} \frac{x_2 - x_1}{f} \right) \right|^2 / \left| \tilde{I}_s(0) \right|^2 d\omega \right]. \end{aligned} \quad (4.19)$$

The result is a spectrally averaged version of the van Cittert–Zernike distribution multiplied by the small factor $1/\Omega T$ and added to a large background term.

E. Polychromatic photon and biphoton diffraction

We now consider a 4- f system, as illustrated in Fig. 2(b), with Fourier-plane aperture of frequency-independent transmittance $t(x)$, so that $h(x_1, x; \omega) = h_s(x_1, x; \omega) = h_i(x_1, x; \omega) = T[(\omega/c)(x - x_1)/f]$ where $T(q)$ is the Fourier transform of $t(x)$. In this case,

$$\begin{aligned} \tilde{G}^{(1)}(x_1, x_2; \omega) &\propto \int I_s(x) T^* \left(\frac{\omega}{c} \frac{x - x_1}{f} \right) \\ &\times T \left(\frac{\omega}{c} \frac{x - x_2}{f} \right) dx \quad (\text{incoherent}), \end{aligned} \quad (4.20)$$

$$\begin{aligned} \tilde{\psi}(x_1, x_2; \omega) &\propto \int E_p(x) T \left(\frac{\omega}{c} \frac{x - x_1}{f} \right) \\ &\times T \left(\frac{\omega_p - \omega}{c} \frac{x - x_2}{f} \right) dx \quad (\text{biphoton}). \end{aligned} \quad (4.21)$$

These expressions may be used to determine the biphoton rates $G^{(2)}$ and C .

In the limit of a narrow source or narrow pump beam, Eq. (4.20) (with the additional assumption that the incoherent source is thermal), and Eq. (4.21) lead to

$$\begin{aligned} C_{\text{th}}(x_1, x_2) &\propto 1 + \frac{1}{T} \int \left| T \left(-\frac{\omega}{c} \frac{x_1}{f} \right) \right|^2 \\ &\times \left| T \left(-\frac{\omega}{c} \frac{x_2}{f} \right) \right|^2 d\omega \quad (\text{incoherent thermal}), \end{aligned} \quad (4.22)$$

$$C(x_1, x_2) \propto \int \left| T\left(-\frac{\omega}{c} \frac{x_1}{f}\right) \right|^2 \times \left| T\left(-\frac{\omega_p - \omega}{c} \frac{x_2}{f}\right) \right|^2 d\omega \quad (\text{biphoton}). \quad (4.23)$$

Note that that neither of these two functions is separable, although the source is a point. This is because the polychromatic source introduces spectral modes that reduce the separability (coherence/entanglement).

In the opposite limit of an extended source, say a uniform source, $I_s(x) = I_0$ and $E_p(x) = E_0$, the coherence function of the incoherent source and the wave function of the biphoton source are least separable. As an example, suppose that all apertures are slits of width D , so that $t(x) = \text{rect}(x/D)$, where $\text{rect}(x)$ is a symmetric rectangular function of unity width. In this case, for the biphoton source,

$$G^{(2)}(x, t_1; x, t_2) = 4G_0 \left[(1 - \rho) \text{sinc}\left(\frac{t_1 - t_2}{\tau_c}\right) - \frac{\rho}{2} \text{sinc}^2\left(\frac{t_1 - t_2}{2\tau_c}\right) \right]^2, \quad (4.24)$$

$$G^{(2)}(x_1, t; x_2, t) = 4 \left(1 - \frac{\rho}{2}\right)^2 \times G_0 \text{sinc}^2\left((2 - \rho) \frac{x_1 - x_2}{x_c}\right) \times \text{sinc}^2\left(\rho \frac{x_1 - x_2}{x_c}\right), \quad (4.25)$$

where $G_0 = 16\pi^4 E_0^2 / x_c^2 \tau_c^2$, $\rho = \Omega / \omega_p$, $\tau_c = 2\pi / \Omega$, $x_c = 4\lambda_p F^\# = 2\lambda_0 F^\#$, and $F^\# = f/D$ is the F number of the lens. The parameter x_c is the resolution of a diffraction-limited incoherent optical system at the degenerate frequency ω_0 . For $\rho \ll 1$, i.e., if a narrow filter centered at the degenerate frequency is used, and in the limit $\rho = 1$,

$$G^{(2)}(x, t_1; x, t_2) = 4G_0 \text{sinc}^2\left(\frac{t_1 - t_2}{\tau_c}\right), \quad \rho \ll 1 \\ = G_0 \text{sinc}^4\left(\frac{t_1 - t_2}{2\tau_c}\right), \quad \rho = 1; \quad (4.26)$$

$$G^{(2)}(x, t_1; x_2, t) = 4G_0 \text{sinc}^2\left(2 \frac{x_1 - x_2}{x_c}\right), \quad \rho \ll 1 \\ = G_0 \text{sinc}^4\left(\frac{x_1 - x_2}{x_c}\right), \quad \rho = 1. \quad (4.27)$$

The temporal width (half width at half maximum value) of the function $G^{(2)}(x, t_1; x, t_2)$ in Eq. (4.24) is $0.44\tau_c$ for a small spectral width ($\rho \ll 1$), and decreases slightly with increase of ρ , reaching a value of $0.42\tau_c$ for $\rho = 0.3$. The spatial width (half width at half maximum value) of the function

$G^{(2)}(x_1, t; x_2, t)$ in Eq. (4.25) increases slightly from $0.22x_c$ to $0.26x_c$ as ρ increases from 0 to 0.3. The function $C(x_1, x_2)$ has approximately the same width as $G^{(2)}(x_1, t; x_2, t)$.

F. Polychromatic photon and biphoton interference

In the special case of a two-slit aperture, $t(x) = \delta(x - a/2) + \delta(x + a/2)$, the previous equations may be used to determine expressions for the interference pattern. In the biphoton case,

$$C(x_1, x_2) \propto 1 + \frac{1}{1 + S_2^2} \left[S_2^2 \mu_+(x_1 - x_2) \cos\left(2\pi \frac{x_1 + x_2}{\Lambda}\right) + \mu_-(x_1 + x_2) \cos\left(2\pi \frac{x_1 - x_2}{\Lambda}\right) \right] + \frac{2S_2}{1 + S_2^2} \left[\mu(x_1) \cos\left(2\pi \frac{x_1}{\Lambda}\right) + \mu(x_2) \cos\left(2\pi \frac{x_2}{\Lambda}\right) \right], \quad (4.28)$$

where $S_2 = \tilde{E}_p(2\pi/\Lambda) / [\int_{-\rho\pi/\Lambda}^{\rho\pi/\Lambda} |\tilde{E}_p(q)|^2 dq]^{1/2}$ and

$$\mu_+(x) = \text{sinc}\left(\rho \frac{x}{\Lambda}\right), \\ \mu_-(x) = \frac{|\int_{-\rho\pi/\Lambda}^{\rho\pi/\Lambda} |\tilde{E}_p(q)|^2 e^{iqx} dq|}{|\int_{-\rho\pi/\Lambda}^{\rho\pi/\Lambda} |\tilde{E}_p(q)|^2 dq|}, \quad (4.29) \\ \mu(x) = \frac{\int_{-\rho\pi/\Lambda}^{\rho\pi/\Lambda} \tilde{E}_p(q) e^{iqx} dq}{[\int_{-\rho\pi/\Lambda}^{\rho\pi/\Lambda} |\tilde{E}_p(q)|^2 dq]^{1/2}}.$$

Here, as before, $\Lambda = 2\pi c / \omega_0 \theta = \lambda_0 / \theta$ is the period of the interference pattern, $\theta = a/f$ is the angle subtended by the pinholes, and $\rho = \Omega / \omega_0$ is the normalized spectral width. In the narrow-band limit, $\rho \rightarrow 0$, $\mu_+(x) = \mu_-(x) = \mu(x) = 1$, and Eq. (4.28) reproduces Eq. (3.8).

In the incoherent case, the single-photon interference pattern is

$$I(x) \propto \left[1 + \mu_{\text{inc}}(x) S_1 \cos\left(2\pi \frac{x}{\Lambda} + \varphi\right) \right], \quad (4.30)$$

where $S_1 = \tilde{I}_s(\Lambda^{-1}) / \tilde{I}_s(0)$ and

$$\mu_{\text{inc}}(x) = \frac{\Lambda}{2\pi\rho} \left| \frac{\int_{2\pi\Lambda^{-1}(1+\rho/2)}^{2\pi\Lambda^{-1}(1-\rho/2)} \tilde{I}_s(q) e^{iqx} dq}{\tilde{I}_s(2\pi\Lambda^{-1})} \right|, \quad (4.31)$$

and φ is a phase factor of no consequence. In the limit $\rho \rightarrow 0$, $\mu_{\text{inc}}(x) = 1$, so that Eq. (4.30) reproduces Eq. (2.9). In general, the interference pattern in Eq. (4.30) has a visibility $V_{\text{inc}} = S_1 \mu_{\text{inc}}(x)$, which has a maximum value $V_{\text{max}} = S_1$ at $x = 0$.

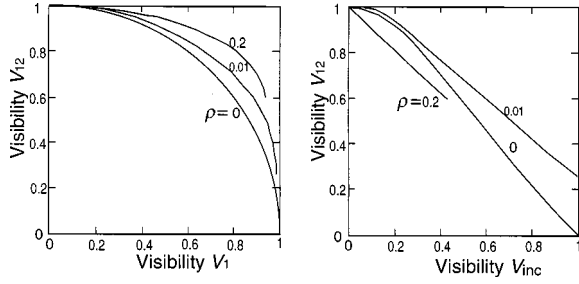


FIG. 5. (a) Visibility V_{12} of pure biphoton fringes versus visibility V_1 of marginal single-photon fringes in a SPDC interference experiment. (b) Visibility V_{12} of pure biphoton fringes in a SPDC interference experiment versus visibility V_{inc} of single photons generated by an equivalent incoherent source. The parameter ρ is the normalized spectral width of the source.

We have computed the two-photon and single-photon visibilities, V_{12} and V_1 , respectively, for the biphoton source, and the visibility V_{inc} for the equivalent incoherent source, and plotted the complementarity and the duality relations for a few values of the normalized spectral width ρ . The results are exhibited in Fig. 5, which is the generalization of Fig. 4 for finite spectra width.

It is of interest to observe that the single complementarity relationship Eq. (3.15) that governs the visibilities of the marginal single-photon and pure biphoton patterns is valid only for monochromatic SPDC light [Fig. 5(a), $\rho=0$].

V. EFFECT OF SOURCE THICKNESS ON PARTIAL COHERENCE AND PARTIAL ENTANGLEMENT

The analogy between the SPDC biphoton source and the conventional incoherent source is also applicable to thick sources, but the nature of the equivalence is somewhat different. We begin with a brief overview of conventional coherence theory for a thick incoherent source and then establish the equivalence with SPDC light generated from a thick nonlinear crystal.

A. Coherence theory for thick polychromatic incoherent sources

A thick source extending between the transverse planes $z = -l$ and $z = 0$ [see Fig. 6(a)] emits incoherently at a photon rate corresponding to the spectral density $I_s(x, z; \omega)$. The emissions from any two points (x, z) and (x', z') are uncorrelated so that the second-order spectral coherence function is

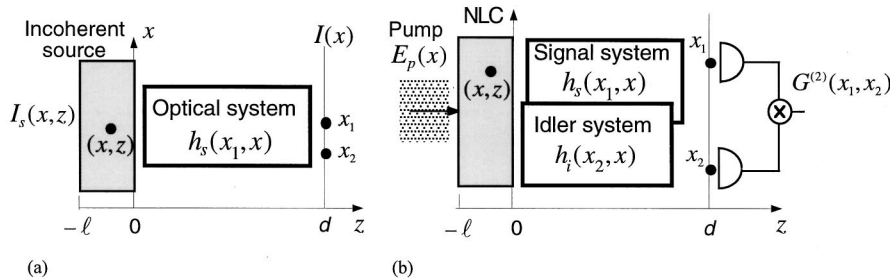


FIG. 6. (a) Light emitted from a thick incoherent source transmitted through an optical system. (b) SPDC light emitted from a thick crystal transmitted through signal and idler systems.

$$\tilde{G}_s^{(1)}(x, z, x', z'; \omega) = I_s(x, z; \omega) \delta(x - x') \delta(z - z'). \quad (5.1)$$

The emitted light is transmitted through a linear system and is observed at points at the plane $z = d > 0$. Propagation between a transverse plane z within the source ($-l < z < 0$) and the observation plane $z = d$ is described by an impulse response function $h_z(x_1, x; \omega)$ at the angular frequency ω , where (x, z) is a point within the source and (x_1, d) is a point in the observation plane. Under these conditions, the second-order spectral coherence function at two points in the observation plane is

$$\tilde{G}^{(1)}(x_1, x_2; \omega) = \iint I_s(x, z; \omega) h_z^*(x_1, x; \omega) \times h_z(x_2, x; \omega) dx dz. \quad (5.2)$$

The system h_z may be segmented as the cascade of a system describing propagation between the plane z within the source and the frontal plane of the source ($z = 0$), followed by a system describing propagation between the source frontal plane and the observation plane. If these systems have impulse response functions $h_z^s(x_1, x; \omega)$ and $h(x_1, x; \omega)$, respectively, we may substitute $h_z(x_1, x; \omega) = \int h(x_1, x'; \omega) h_z^s(x', x; \omega) dx'$ into Eq. (5.2) and obtain

$$\tilde{G}^{(1)}(x_1, x_2; \omega) = \iint \Gamma_s(x', x''; \omega) h^*(x_1, x'; \omega) \times h(x_2, x''; \omega) dx' dx'', \quad (5.3)$$

where

$$\Gamma_s(x', x''; \omega) = \iint I_s(x, z; \omega) h_z^{s*}(x', x; \omega) \times h_z^s(x'', x; \omega) dx dz. \quad (5.4)$$

Equation (5.3) describes the propagation of partially coherent light with spectral coherence function $\Gamma_s(x, x'; \omega)$ between the planes $z = 0$ and $z = d$.

It follows that a thick incoherent source may be replaced with an equivalent partially coherent thin planar source. This is not surprising since partial coherence is acquired as a result of propagation of light emitted incoherently within the

source to the frontal plane of the source. Equation (5.3) may also be translated to the spatial Fourier domain,

$$\begin{aligned} \tilde{G}^{(1)}(x_1, x_2; \omega) &= \frac{1}{4\pi^2} \int \int \tilde{\Gamma}_s(-q_1, q_2; \omega) H^*(x_1, q_1; \omega) \\ &\quad \times H(x_2, q_2; \omega) dq_1 dq_2, \end{aligned} \quad (5.5)$$

where $\tilde{\Gamma}_s(q_1, q_2; \omega)$ is the two-dimensional Fourier transform of $\Gamma_s(x', x''; \omega)$.

B. Entanglement theory for thick polychromatic biphoton sources

We now consider spontaneous parametric down-conversion from a thick crystal of width l pumped by a monochromatic beam of angular frequency ω_p and amplitude $E_p(x)$, as illustrated in Fig. 6(b). The signal and idler beams are transmitted through linear systems of impulse response functions $h_s(x_1, x; \omega)$ and $h_i(x_2, x; \omega)$, respectively, at the angular frequency ω . It is shown in the Appendix that the spectral wave function at the output of these systems (the observation plane) is given by

$$\begin{aligned} \tilde{\psi}(x_1, x_2; \omega) &= \int \int \Gamma(x', x''; \omega) h_s(x_1, x'; \omega) \\ &\quad \times h_i(x_2, x''; \omega_p - \omega) dx' dx'' \end{aligned} \quad (5.6)$$

or

$$\begin{aligned} \tilde{\psi}(x_1, x_2; \omega) &= \frac{1}{4\pi^2} \int \int \Lambda(q_s, q_i; \omega) H_s(x_1, q_s; \omega) \\ &\quad \times H_i(x_2, q_i; \omega_p - \omega) dq_s dq_i, \end{aligned} \quad (5.7)$$

where $H_s(x_1, q_s; \omega)$ is the Fourier transform of $h_s(x_1, x; \omega)$ with respect to the variable x , and similarly for the idler system. The kernels Γ and Λ in Eqs. (5.6) and (5.7) are related to the pump distribution by

$$\Gamma(x', x''; \omega_s) = \int E_p(x) \zeta(x+x', x+x''; \omega_s) dx \quad (5.8)$$

and

$$\Lambda(q_s, q_i; \omega) = \tilde{E}_p(q_s + q_i) \tilde{\zeta}(q_s, q_i; \omega), \quad (5.9)$$

where

$$\tilde{\zeta}(q_s, q_i; \omega_s) = l \operatorname{sinc}\left(\frac{l}{2\pi} \Delta r\right) \exp\left(-j \frac{l}{2} \Delta r\right) \quad (5.10)$$

with $\Delta r = r_p - r_s - r_i$ and $r = \sqrt{n^2(\omega) \omega^2 / c^2 - q^2}$. The quantity $\tilde{\zeta}(q_s, q_i; \omega_s)$ is related to the crystal parameters and $\zeta(x', x''; \omega_s)$ is its inverse Fourier transform. Using the above expression for the spectral wave function, the wave function $\psi(x_1, t_1, x_2, t_2)$ and the biphoton rate $C(x_1, x_2)$ may be readily determined by the use of Eqs. (4.11) and (4.14).

The structure of Eq. (5.6) is identical to that for partially coherent imaging, Eq. (5.3), with the function $\Gamma(x', x''; \omega_s)$

playing the role of the source coherence function $\Gamma_s(x', x''; \omega)$. It follows that SPDC light generated by a thick crystal is similar to partially coherent light emitted by a planar surface, or incoherent light emitted by a thick source.

In the special case of a uniform pump of unity amplitude, Eq. (5.8) simplifies to

$$\Gamma(x', x''; \omega_s) = \int \zeta(x+x', x+x''; \omega_s) dx \equiv \gamma(x' - x''; \omega_s), \quad (5.11)$$

where $\gamma(x, \omega_s)$ is the inverse Fourier transform of $\tilde{\zeta}(q_s, -q_s; \omega_s)$. In this case, the source function is homogeneous, as expected for a uniform pump and a crystal of infinite transverse spatial extent. The function $\gamma(x; \omega_s)$ is entirely determined by the thickness and dispersive properties of the nonlinear crystal at the signal and idler frequencies.

C. van Cittert-Zernike theorems for thick polychromatic photon and biphoton sources

For the 2- f system shown in Fig. 2(a), $H_s(x_1, q; \omega) = H_i(x_1, q; \omega) \propto d[q - (\omega/c)(x_1/f)]$ so that Eq. (5.7) gives

$$\begin{aligned} \tilde{\psi}(x_1, x_2; \omega_s) &\propto \tilde{E}_p \left(\frac{\omega_s x_1}{c f} + \frac{\omega_p - \omega_s x_2}{c f} \right) \\ &\quad \times \zeta \left(\frac{\omega_s x_1}{c f}, \frac{\omega_p - \omega_s x_2}{c f}; \omega_s \right). \end{aligned} \quad (5.12)$$

Equation (5.12) is a generalization of Eq. (4.16). The biphoton rate is determined from Eq. (5.12) by use of Eqs. (4.10) and (4.11) or (4.14). Here, the spatial Fourier transform of the pump distribution, which appears in the previously derived biphoton van Cittert-Zernike theorem, is multiplied by a factor ζ representing the degree of phase matching permitted by the thickness of the nonlinear crystal.

D. Biphoton diffraction for a thick polychromatic biphoton source

If the signal and idler systems are 4- f systems with apertures of frequency-independent transmittances $t_s(x)$ and $t_i(x)$ placed in the Fourier plane, as shown in Fig. 2(b), then $H_s(x, q; \omega) \propto e^{-ixq} t_s[(cf/\omega)q]$ and $H_i(x, q; \omega) \propto e^{-ixq} t_i[(cf/\omega)q]$, so that

$$\begin{aligned} \tilde{\psi}(x_1, x_2; \omega_s) &\propto \int \int e^{-i(q_s x_1 + q_i x_2)} \tilde{\zeta}(q_s, q_i; \omega_s) \tilde{E}_p(q_s + q_i) \\ &\quad \times t_s\left(\frac{cf}{\omega_s} q_s\right) t_i\left(\frac{cf}{\omega_p - \omega_s} q_i\right) dq_s dq_i. \end{aligned} \quad (5.13)$$

For a uniform pump

$$\begin{aligned} \tilde{\psi}(x_1, x_2; \omega_s) &\propto \int e^{-iq_s(x_1 - x_2)} \tilde{\zeta}(q_s, -q_s; \omega_s) t_s \\ &\quad \times \left(\frac{cf}{\omega_s} q_s \right) t_i \left(\frac{-cf}{\omega_p - \omega_s} q_s \right) dq_s. \end{aligned} \quad (5.14)$$

We have evaluated the integral in Eq. (5.14) numerically and used Eqs. (4.11) and (4.10) to determine the biphoton rate $G^{(2)}(x, t_1, x, t_2)$ as a function of the time separation $t_1 - t_2$, and the rate $C(x_1, x_2)$ of Eq. (4.14) as a function of the spatial separation $x_1 - x_2$ for 4- f signal and idler systems with aperture functions $t_s(x) = t_i(x) = \text{rect}(x/D)$, corresponding to diffraction-limited imaging with a lens of F number $F^\# = f/D = 5$. The pump was assumed to be uniform and monochromatic and to have a wavelength $\lambda_p = 325$ nm. The parameters for a beta-barium-borate (BBO) crystal in a type-I configuration were assumed in the calculation [$n_e(\omega_p) = 1.667$ at an angle of 36.44° and $n_o(\omega_s) = n_o(\omega_i)$ were determined by use of the Sellmeier equations]. Three crystal widths, $l = 0.1, 1, \text{ and } 10$ mm, were used. Filters of width $\Omega = 0.05\omega_p$ centered at the degenerate frequency $\omega_0 = \omega_p/2$ were used in both the signal and idler beams (i.e., $\rho = 0.05$). The results are displayed in Fig. 7. The values obtained when the crystal width is $l = 0.1$ mm are approximately the same as those predicted for the thin-crystal limit (Sec. IV).

The widths (half width at half maximum values) of the functions $C(x_1, x_2)$ shown in Fig. 7(a), are approximately $0.27x_c$, $0.85x_c$, and $2.0x_c$ for $l = 0.1, 1, \text{ and } 10$ mm, respectively. In the thin-crystal limit, this width is $0.23x_c$. Thus the width of $C(x_1, x_2)$, which determines the fourth-order coherence area, increases significantly with increase of the crystal thickness. The temporal widths (half width at half maximum values) of the functions $G^{(2)}(x, t_1; x, t_2)$, which are shown in Fig. 7(b), are approximately $0.44\tau_c$, $0.43\tau_c$, and $0.53\tau_c$ for $l = 0.1, 1, \text{ and } 10$ mm, respectively. In the thin-crystal limit, that width is $0.44\tau_c$. Thus the width of $G^{(2)}(x, t_1, x, t_2)$, which determines the fourth-order coherence time, is relatively insensitive to the crystal thickness.

VI. CONCLUSION

The emission of pairs of photons (biphotons) from a nonlinear crystal illuminated by a pump wave in a spontaneous parametric down-conversion process is analogous to the spontaneous emission of single photons from a conventional incoherent source. The uncorrelated nature of the emissions from different points of the source, whether single photons or entangled-photon pairs, governs the process of propagation of the emitted light through optical systems. The two-particle wave function in the biphoton case is analogous to the second-order coherence function in the incoherent case, and the pump spatial profile is analogous to the source intensity distribution. With this analogy, it has been established in this paper that the phenomena of diffraction, interference, and growth of coherence in conventional optics have their counterparts in biphoton optics. This similarity is applicable for quasimonochromatic and broadband light, and for both thin and thick sources.

The underlying mathematical similarity between the two theories results in a duality between the theory of partial coherence in conventional sources and partial entanglement in sources of spontaneous parametric down-conversion. Since the process of spontaneous parametric down-conversion is governed by conservation of energy and mo-

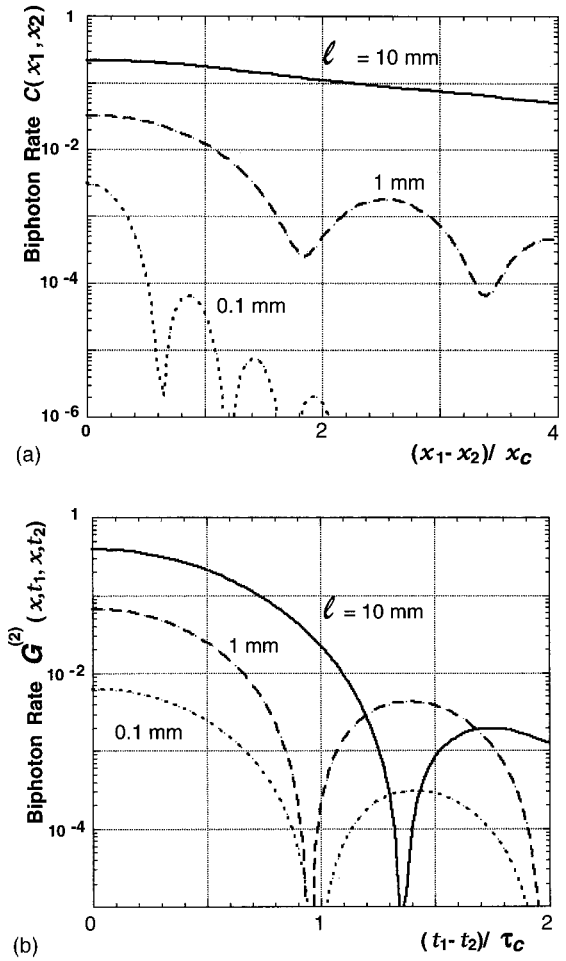


FIG. 7. Biphoton rates (in arbitrary units) at the output of a 4- f optical system for a SPDC source using a crystal with thickness l and spectral width $\Omega = 0.05\omega_p$ (i.e., $\rho = 0.05$). The system uses a lens of F number $F^\# = 5$. (a) Dependence of the biphoton rate $C(x_1, x_2)$ on the separation $(x_1 - x_2)$ normalized to the resolution length $x_c = 2\lambda_0 F^\#$. (b) Dependence of the biphoton rate $G^{(2)}(x, t_1, x, t_2)$ on the time delay $(t_1 - t_2)$ normalized to the inverse spectral width $\tau_c = 2\pi/\Omega$.

mentum, the emitted light exhibits spatial and spectral entanglement. The larger the size of the pump, the less separable the two-photon wave function, and the greater the entanglement. In the dual world of spontaneous emission from a conventional incoherent source, the smaller the source, the more separable the coherence function of the emitted light, and the more coherent the emission. Thus, nonseparability of the joint wave function, which is the essence of entanglement in the biphoton case, corresponds to the absence of coherence in the conventional case. Separability is associated with nonentanglement in one world, and with coherence in the other.

This duality means that, for an optical system illuminated by a conventional source with geometry such that the transmitted light is of greater coherence, the dual biphoton system will manifest lower entanglement. As an interferometer, the former system produces ordinary interference fringes with

higher visibility, whereas the latter will reveal biphoton interference fringes of lower visibility. As the geometry of the system is altered to reduce coherence (fringe visibility) in the conventional case, increased entanglement (fringe visibility) will emerge in the dual biphoton case.

ACKNOWLEDGMENTS

The authors thank Bradley Jost and Michael Horne for valuable discussions. This work was supported by the National Science Foundation.

APPENDIX

Expressions for the SPDC biphoton state $|\psi\rangle$ are derived under various conditions.

The simplest theory, used in Sec. III, is applicable for a thin planar crystal under quasimonochromatic conditions. Here, the biphoton state is written as

$$|\Psi\rangle = \int \int dx dx' E_p(x) \delta(x-x') \hat{a}_s^\dagger(x) \hat{a}_i^\dagger(x') |0,0\rangle, \quad (\text{A1})$$

where $|0,0\rangle$ is the vacuum state, \hat{a}_s^\dagger and \hat{a}_i^\dagger are creation operators for the signal and idler modes, respectively, and $E_p(x)$ is the electric field of the pump, which is assumed to be classical and controls the rate of down-conversion. This function is also affected by the aperture of the nonlinear crystal if the pump is not confined within the crystal. The operators for the positive-frequency portions of the signal and idler electric fields at the detection plane are expressed in terms of the annihilation operators $\hat{a}_s(x)$ and $\hat{a}_i(x)$ at the source plane (the crystal) and the impulse response functions of the signal and idler systems:

$$\begin{aligned} \hat{E}_1^+(x_1) &= \int h_s(x_1, x) \hat{a}_s(x) dx, \\ \hat{E}_2^+(x_2) &= \int h_i(x_2, x) \hat{a}_i(x) dx. \end{aligned} \quad (\text{A2})$$

By simple substitution, it follows that the wave function $\psi(x_1, x_2) = \langle 0,0 | \hat{E}_2^+(x_2) \hat{E}_1^+(x_1) | \Psi \rangle$ is related to the pump distribution and the system functions by Eq. (3.4).

We now consider the more general case of a thick crystal, and include temporal and spectral effects. We express the state of the emitted biphoton in the wave-vector domain by

$$|\Psi\rangle = \int \int d\mathbf{k}_s d\mathbf{k}_i \Phi(\mathbf{k}_s, \mathbf{k}_i) \hat{a}^\dagger(\mathbf{k}_s) \hat{a}^\dagger(\mathbf{k}_i) |0,0\rangle, \quad (\text{A3})$$

where $\hat{a}^\dagger(\mathbf{k}_s)$ and $\hat{a}^\dagger(\mathbf{k}_i)$ are the photon creation operators for signal and idler waves of wave vectors \mathbf{k}_s and \mathbf{k}_i , respectively, and $\Phi(\mathbf{k}_s, \mathbf{k}_i)$ is a function representing the coupling between the wave vectors, which results from the conservation of energy and momentum that are inherent in the parametric process. The emitted signal and idler waves travel through the signal and idler optical systems and create the field operators

$$\hat{E}_1^+(x, t) = \int d\mathbf{k}_s H_s(x, \mathbf{k}_s) e^{-i\omega_s t} \hat{a}_{\mathbf{k}_s}, \quad (\text{A4})$$

$$\hat{E}_2^+(x, t) = \int d\mathbf{k}_i H_i(x, \mathbf{k}_i) e^{-i\omega_i t} \hat{a}_{\mathbf{k}_i}$$

at the detection plane, where the \hat{a} are the photon annihilation operators. Each field is a superposition of contributions from the plane waves emitted by the source, each weighted by factors determined by the systems. The factor $H_s(x, \mathbf{k}_s)$ is the response of the signal system at position x when illuminated by a monochromatic plane wave of wave vector \mathbf{k}_s and unit amplitude; $H_i(x, \mathbf{k}_i)$ has a similar meaning for the idler wave. The wave function $\psi(x_1, t_1; x_2, t_2) = \langle 0,0 | \hat{E}_2^+(x_2, t_2) \hat{E}_1^+(x_1, t_1) | \Psi \rangle$ at positions x_1 and x_2 and times t_1 and t_2 is then

$$\begin{aligned} \psi(x_1, t_1; x_2, t_2) &= \int \int e^{-i(\omega_s t_1 + \omega_i t_2)} \Phi(\mathbf{k}_s, \mathbf{k}_i) \\ &\times H_s(x_1, \mathbf{k}_s) H_i(x_2, \mathbf{k}_i) d\mathbf{k}_s d\mathbf{k}_i. \end{aligned} \quad (\text{A5})$$

Using a plane-wave expansion of the pump wave $\tilde{E}_p(\mathbf{k}_p)$, we express $\Phi(\mathbf{k}_s, \mathbf{k}_i)$ in the form

$$\Phi(\mathbf{k}_s, \mathbf{k}_i) = \int d\mathbf{k}_p \tilde{E}_p(\mathbf{k}_p) \xi(\mathbf{k}_p - \mathbf{k}_s - \mathbf{k}_i) \delta(\omega - \omega_s - \omega_i), \quad (\text{A6})$$

where perfect energy conservation is represented by the δ function, whereas $\xi(\cdot)$ represents the imperfect phase matching that results from the finite size of the parametric interaction volume. The angular frequencies ω_s , ω_i , and ω correspond to the wave vectors \mathbf{k}_s , \mathbf{k}_i , and \mathbf{k}_p , respectively. Since the finite size of the crystal in the transverse direction is equivalent to a pump with finite aperture, and since we assume that the pump is of arbitrary transverse distribution, there is no loss of generality in assuming that the crystal is infinite in the transverse direction.

Equations (A4) and (A5) are simplified by replacing the wave vector \mathbf{k} with the transverse component q (which is assumed, for simplicity, to be one dimensional) and the corresponding frequency ω . Thus the vector \mathbf{k} will be replaced by the two scalars (q, ω) . For example, $H_s(x_1, \mathbf{k}_s)$ will be denoted as $H_s(x_1, q_s; \omega_s)$, and so on. If the signal system is characterized by its spatial impulse response function $h_s(x_1, x; \omega_s)$ at the angular frequency ω_s , then $H_s(x_1, q_s, \omega_s)$ is simply the spatial Fourier transform of $h_s(x_1, x, \omega_s)$ with respect to the variable $-x$. Similar relations apply to the idler system. We assume that the pump is a monochromatic beam of angular frequency ω_p and amplitude $E_p(x)$, so that

$$\tilde{E}_p(\mathbf{k}_p) = \tilde{E}_p(q) \delta(\omega - \omega_p), \quad (\text{A7})$$

where $\tilde{E}_p(q)$ is the Fourier transform of $E_p(x)$, the pump spatial distribution at the input face of the crystal.

We first consider the limit of a thin crystal (relating to Sec. IV) and then generalize the results to a crystal of arbitrary thickness (relating to Sec. V). For a sufficiently thin crystal, the phase-matching condition is applicable only in the transverse direction, so that

$$\xi(\mathbf{k}_p - \mathbf{k}_s - \mathbf{k}_i) = \delta(q_p - q_s - q_i), \quad (\text{A8})$$

where q_s , q_i , and q_p are the transverse components of the wave vectors \mathbf{k}_s , \mathbf{k}_i , and \mathbf{k}_p , respectively. The combination of Eqs. (A5)–(A8) then leads to the biphoton wave function given in Eqs. (4.11) and (4.13). Using Fourier-transform relations leads to Eq. (4.12).

We now consider the effect of finite thickness of the nonlinear crystal. For a crystal of thickness l in the longitudinal direction, but infinite extent in the transverse direction, the phase-matching function is

$$\xi(\mathbf{k}_p - \mathbf{k}_s - \mathbf{k}_i) = \delta(q_p - q_s - q_i) l \operatorname{sinc}\left(\frac{l}{2\pi}(\Delta r)\right) \times \exp\left(-j\frac{l}{2}\Delta r\right), \quad (\text{A9})$$

where $\Delta r = r_p - r_s - r_i$ and $r = \sqrt{n^2(\omega)\omega^2/c^2 - q^2}$ is the longitudinal component of a wave vector \mathbf{k} of transverse component q , angular frequency ω , and refractive index $n(\omega)$. As before, the subscripts p , s , and i denote the pump, signal, and idler, respectively. Therefore, for a monochromatic pump of frequency ω_p ,

$$\xi(\mathbf{k}_p - \mathbf{k}_s - \mathbf{k}_i) = \delta(q_p - q_s - q_i) \tilde{\zeta}(q_s, q_i; \omega_s), \quad (\text{A10})$$

where $\tilde{\zeta}(q_s, q_i; \omega_s)$ is given by Eq. (5.10). Substituting Eq. (A10) into Eqs. (A6) and (A5) leads to Eqs. (5.7)–(5.9).

-
- [1] W. H. Louisell, A. Yariv, and A. E. Siegman, *Phys. Rev.* **124**, 1646 (1961); J. P. Gordon, W. H. Louisell, and L. R. Walker, *ibid.* **129**, 481 (1963).
- [2] D. N. Klyshko, *Pis'ma Zh. Eksp. Teor. Fiz.* **6**, 490 (1967) [*JETP Lett.* **6**, 23 (1967)]; *Zh. Eksp. Teor. Fiz.* **55**, 1006 (1968) [*Sov. Phys. JETP* **28**, 522 (1969)]; T. G. Giallorenzi and C. L. Tang, *Phys. Rev.* **166**, 225 (1968); D. A. Kleiman, *ibid.* **174**, 1027 (1968).
- [3] D. N. Klyshko, *Photons and Nonlinear Optics* (Nauka, Moscow, 1980), Chaps. 1, 6 (translation: Gordon and Breach, New York, 1988).
- [4] A. Yariv, *Quantum Electronics*, 3rd ed. (Wiley, New York, 1988), Chap. 17; B. E. A. Saleh and M. C. Teich, *Fundamentals of Photonics* (Wiley, New York, 1991), Chaps. 10, 19; J. Peřina, Z. Hradil, and B. Jurčo, *Quantum Optics and Fundamentals of Physics* (Kluwer, Boston, 1994), Chaps. 2, 7, 8; L. Mandel and E. Wolf, *Optical Coherence and Quantum Optics* (Cambridge, New York, 1995), Chap. 22.
- [5] S. E. Harris, M. K. Oshman, and R. L. Byer, *Phys. Rev. Lett.* **18**, 732 (1967); R. L. Byer and S. E. Harris, *Phys. Rev.* **168**, 1064 (1968); D. Magde and H. Mahr, *Phys. Rev. Lett.* **18**, 905 (1967); D. N. Klyshko and D. P. Krindach, *Zh. Eksp. Teor. Fiz.* **54**, 697 (1968) [*Sov. Phys. JETP* **27**, 371 (1968)]; K. Koch, E. C. Cheung, G. T. Moore, S. H. Chakmakjian, and J. M. Liu, *IEEE J. Quantum Electron.* **31**, 769 (1995).
- [6] B. Ya. Zel'dovich and D. N. Klyshko, *Pis'ma Zh. Eksp. Teor. Fiz.* **9**, 69 (1969) [*JETP Lett.* **9**, 40 (1969)]; B. R. Mollow, *Phys. Rev. A* **8**, 2684 (1973); C. K. Hong and L. Mandel, *ibid.* **31**, 2409 (1985).
- [7] D. N. Klyshko, *Kvant. Electron. (Moscow)* **4**, 1056 (1977) [*Sov. J. Quantum Electron.* **7**, 591 (1977)].
- [8] D. C. Burnham and D. L. Weinberg, *Phys. Rev. Lett.* **25**, 84 (1970); S. Friberg, C. K. Hong, and L. Mandel, *ibid.* **54**, 2011 (1985); C. K. Hong, Z. Y. Ou, and L. Mandel, *ibid.* **59**, 2044 (1987).
- [9] T. S. Larchuk, M. C. Teich, and B. E. A. Saleh, *Ann. (N.Y.) Acad. Sci.* **755**, 680 (1995); P. R. Tapster and J. G. Rarity, *J. Mod. Opt.* **45**, 595 (1998).
- [10] E. Schrödinger, *Naturwissenschaften* **23**, 807 (1935); **23**, 823 (1935); **23**, 844 (1935) [translation: J. D. Trimmer, *Proc. Am. Philos. Soc.* **124**, 323 (1980); reprinted in *Quantum Theory and Measurement*, edited by J. A. Wheeler and W. H. Zurek (Princeton University Press, Princeton, NJ, 1983)].
- [11] M. H. Rubin, D. N. Klyshko, Y. H. Shih, and A. V. Sergienko, *Phys. Rev. A* **50**, 5122 (1994); M. Atatüre, A. V. Sergienko, B. E. A. Saleh, and M. C. Teich, *Phys. Rev. Lett.* **84**, 618 (2000).
- [12] A. Einstein, B. Podolsky, and N. Rosen, *Phys. Rev.* **47**, 777 (1935); N. Bohr, *Nature (London)* **121**, 65 (1935); *Phys. Rev.* **48**, 696 (1935); J. S. Bell, *Physics (Long Island City, N.Y.)* **1**, 195 (1964); *Rev. Mod. Phys.* **38**, 447 (1966); in *Foundations of Quantum Mechanics*, Proceedings of the International School of Physics "Enrico Fermi," Course IL (Academic, New York, 1971), pp. 171–181; in Proceedings of the Symposium on Frontier Problems in High Energy Physics, *Pisa, 1976*, pp. 35–45; *Int. J. Quantum Chem., Quantum Chem. Symp.* **14**, 155 (1980); J. F. Clauser, M. A. Horne, A. Shimony, and R. A. Holt, *Phys. Rev. Lett.* **23**, 880 (1969).
- [13] C. O. Alley and Y. H. Shih, in *Proceedings of the 2nd International Symposium on Foundations of Quantum Mechanics in Light of New Technology, Tokyo, 1986*, edited by M. Namiki (Physical Society of Japan, Tokyo, 1987), pp. 47–52; Z. Y. Ou and L. Mandel, *Phys. Rev. Lett.* **61**, 50 (1988); Y. H. Shih and C. O. Alley, *ibid.* **61**, 2921 (1988); P. G. Kwiat, K. Mattle, H. Weinfurter, A. Zeilinger, A. V. Sergienko, and Y. H. Shih, *ibid.* **75**, 4337 (1995).
- [14] D. M. Greenberger, M. A. Horne, and A. Zeilinger, in *Bell's Theorem, Quantum Theory, and Conceptions of the Universe*, edited by M. Kafatos (Kluwer, Dordrecht, 1989); D. M. Greenberger, M. A. Horne, A. Shimony, and A. Zeilinger, *Am. J. Phys.* **58**, 1131 (1990); D. Bouwmeester, J.-W. Pan, M. Daniell, H. Weinfurter, and A. Zeilinger, *Phys. Rev. Lett.* **82**, 1345 (1999).
- [15] G. Kh. Kitaeva, A. N. Penin, V. V. Fadeev, and Yu. A. Yanait, *Dokl. Akad. Nauk. SSSR* **247**, 586 (1979) [*Sov. Phys. Dokl.* **24**, 564 (1979)]; A. Migdall, R. Datla, A. Sergienko, J. S. Orszak, and Y. H. Shih, *Appl. Opt.* **37**, 3455 (1998); A. Migdall, *Phys. Today* **52(1)**, 41 (1999).
- [16] D. N. Klyshko, *Kvant. Electron. (Moscow)* **7**, 1932 (1980)

- [Sov. J. Quantum Electron. **10**, 1112 (1980)]; A. A. Malygin, A. N. Penin, and A. V. Sergienko, Pis'ma Zh. Eksp. Teor. Fiz. **33**, 493 (1981) [JETP Lett. **33**, 477 (1981)]; A. N. Penin and A. V. Sergienko, Appl. Opt. **30**, 3582 (1991); A. Migdall, R. Datla, A. V. Sergienko, and Y. H. Shih, Metrologia **32**, 479 (1995).
- [17] E. Jakeman and J. G. Rarity, Opt. Commun. **59**, 219 (1986); M. M. Hayat, A. Joobeur, and B. E. A. Saleh, J. Opt. Soc. Am. A **16**, 348 (1999).
- [18] E. Dauler, G. Jaeger, A. Muller, A. Migdall, and A. Sergienko, J. Res. Natl. Inst. Stand. Technol. **104**, 1 (1999).
- [19] L. Mandel, J. Opt. Soc. Am. B **1**, 108 (1984); C. K. Hong, S. R. Friberg, and L. Mandel, Appl. Opt. **24**, 3877 (1985).
- [20] J. G. Rarity, P. R. Tapster, J. G. Walker, and S. Seward, Appl. Opt. **29**, 2939 (1990).
- [21] H.-B. Fei, B. M. Jost, S. Popescu, B. E. A. Saleh, and M. C. Teich, Phys. Rev. Lett. **78**, 1679 (1997); B. E. A. Saleh, B. M. Jost, H.-B. Fei, and M. C. Teich, *ibid.* **80**, 3483 (1998).
- [22] A. K. Ekert, Phys. Rev. Lett. **67**, 661 (1991); A. K. Ekert, J. G. Rarity, P. R. Tapster, and G. M. Palma, *ibid.* **69**, 1293 (1992); J. Rarity and P. Tapster, J. Defence Sci. **1**, 388 (1996); J. Brendel, N. Gisin, W. Tittel, and H. Zbinden, Phys. Rev. Lett. **82**, 2594 (1999); A. V. Sergienko, M. Atatüre, Z. Walton, G. Jaeger, B. E. A. Saleh, and M. C. Teich, Phys. Rev. A **60**, R2622 (1999); T. Jennewein, C. Simon, G. Weihs, H. Weinfurter, and A. Zeilinger, Phys. Rev. Lett. **84**, 4729 (2000); D. S. Naik, C. G. Peterson, A. G. White, A. J. Berglund, and P. G. Kwiat, *ibid.* **84**, 4733 (2000); W. Tittel, J. Brendel, H. Zbinden, and N. Gisin, *ibid.* **84**, 4737 (2000).
- [23] C. H. Bennett, G. Brassard, C. Crepeau, R. Jozsa, A. Peres, and W. K. Wootters, Phys. Rev. Lett. **70**, 1895 (1993); D. Bouwmeester, J.-W. Pan, K. Mattle, M. Eibl, H. Weinfurter, and A. Zeilinger, Nature (London) **390**, 575 (1997); D. Boschi, S. Branca, F. De Martini, L. Hardy, and S. Popescu, Phys. Rev. Lett. **80**, 1121 (1998).
- [24] J. H. Shapiro and K. X. Sun, J. Opt. Soc. Am. B **11**, 1130 (1994).
- [25] C. K. Hong, Z. Y. Ou, and L. Mandel, Phys. Rev. Lett. **59**, 2044 (1987); R. A. Campos, B. E. A. Saleh, and M. C. Teich, Phys. Rev. A **40**, 1371 (1989); J. D. Franson, Phys. Rev. Lett. **62**, 2205 (1989); Z. Y. Ou, X. Y. Zou, L. J. Wang, and L. Mandel, *ibid.* **65**, 321 (1990); P. G. Kwiat, W. A. Vareka, C. K. Hong, H. Nathel, and R. Y. Chiao, Phys. Rev. A **41**, 2910 (1990); J. G. Rarity, P. R. Tapster, E. Jakeman, T. S. Larchuk, R. A. Campos, M. C. Teich, and B. E. A. Saleh, Phys. Rev. Lett. **65**, 1348 (1990); J. G. Rarity and P. R. Tapster, Phys. Rev. A **41**, 5139 (1990); Z. Y. Ou, X. Y. Zou, L. J. Wang, and L. Mandel, *ibid.* **42**, 2957 (1990); R. A. Campos, B. E. A. Saleh, and M. C. Teich, *ibid.* **42**, 4127 (1990); J. Brendel, E. Mohler, and W. Martienssen, Phys. Rev. Lett. **66**, 1142 (1991); T. S. Larchuk, R. A. Campos, J. G. Rarity, P. R. Tapster, E. Jakeman, B. E. A. Saleh, and M. C. Teich, *ibid.* **70**, 1603 (1993); P. G. Kwiat, A. M. Steinberg, and R. Y. Chiao, Phys. Rev. A **47**, R2472 (1993); Y. H. Shih, A. V. Sergienko, M. H. Rubin, T. E. Kiess, and C. O. Alley, *ibid.* **49**, 4243 (1994).
- [26] A. V. Belinsky and D. N. Klyshko, Phys. Lett. A **166**, 303 (1992).
- [27] D. N. Klyshko, Zh. Eksp. Teor. Fiz. **83**, 1313 (1982) [Sov. Phys. JETP **56**, 753 (1982)]; A. A. Malygin, A. N. Penin, and A. V. Sergienko, Dokl. Akad. Nauk SSSR **281**, 308 (1985) [Sov. Phys. Dokl. **30**, 227 (1985)]; D. N. Klyshko, Zh. Eksp. Teor. Fiz. **94**, 82 (1988) [Sov. Phys. JETP **67**, 1131 (1988)]; A. V. Belinskii and D. N. Klyshko, *ibid.* **105**, 487 (1994) [JETP **78**, 259 (1994)]; D. V. Strekalov, A. V. Sergienko, D. N. Klyshko, and Y. H. Shih, Phys. Rev. Lett. **74**, 3600 (1995); T. B. Pittman, Y. H. Shih, D. V. Strekalov, and A. V. Sergienko, Phys. Rev. A **52**, R3429 (1995); T. B. Pittman, D. V. Strekalov, D. N. Klyshko, M. H. Rubin, A. V. Sergienko, and Y. H. Shih, *ibid.* **53**, 2804 (1996); M. H. Rubin, *ibid.* **54**, 5349 (1996).
- [28] R. Ghosh and L. Mandel, Phys. Rev. Lett. **59**, 1903 (1987).
- [29] A. Joobeur, B. E. A. Saleh, and M. C. Teich, Phys. Rev. A **50**, 3349 (1994); A. Joobeur, B. E. A. Saleh, T. S. Larchuk, and M. C. Teich, *ibid.* **53**, 4360 (1996); B. E. A. Saleh, A. Joobeur, and M. C. Teich, *ibid.* **57**, 3991 (1998).
- [30] T. P. Grayson and G. A. Barbosa, Phys. Rev. A **49**, 2948 (1994); P. H. S. Ribeiro, S. Pádua, J. C. Machado da Silva, and G. A. Barbosa, *ibid.* **49**, 4176 (1994); P. H. S. Ribeiro, C. H. Monken, and G. A. Barbosa, Appl. Opt. **33**, 352 (1994); C. H. Monken, P. H. S. Ribeiro, and S. Pádua, Phys. Rev. A **57**, 3123 (1998).
- [31] J. Řeháček and J. Peřina, Opt. Commun. **125**, 82 (1996).
- [32] B. E. A. Saleh, S. Popescu, and M. C. Teich, in *Proceedings of the Ninth Annual Meeting of IEEE Lasers and Electro-Optics Society*, edited by P. Zory (IEEE, Piscataway, NJ, 1996), Vol. 1, pp. 362–363.
- [33] M. C. Teich and B. E. A. Saleh, Cesk. Cas. Fyz. **47**, 3 (1997); US Patent No. 5,796,477 (18 Aug. 1998).
- [34] B. M. Jost, A. V. Sergienko, A. F. Abouraddy, B. E. A. Saleh, and M. C. Teich, Opt. Express **3**, 81 (1998).
- [35] J. Peřina, *Coherence of Light*, 2nd ed. (Reidel, Boston, 1985); *Quantum Statistics of Linear and Nonlinear Optical Phenomena*, 2nd ed. (Kluwer, Boston, 1991).
- [36] R. J. Glauber, Phys. Rev. **130**, 2529 (1963); R. J. Glauber, *ibid.* **131**, 2766 (1963).
- [37] B. E. A. Saleh, *Photoelectron Statistics* (Springer, New York, 1978).
- [38] O. Steuernagel and H. Rabitz, Opt. Commun. **154**, 285 (1998).
- [39] M. A. Horne, A. Shimony, and A. Zeilinger, Phys. Rev. Lett. **62**, 2209 (1989); G. Jaeger, M. A. Horne, and A. Shimony, Phys. Rev. A **48**, 1023 (1993); G. Jaeger, A. Shimony, and L. Vaidman, Phys. Rev. A **51**, 54 (1995); M. Horne, in *Experimental Metaphysics*, edited by R. S. Cohen, M. Horne, and J. Stachel (Kluwer, Boston, 1997), pp. 109–119.